Coherent versus incoherent light scattering from a quantum dot

K. Konthasinghe,[1] J. Walker,[1] M. Peiris,[1] C. K. Shih,[2] Y. Yu,[3] M. F. Li,[3] J. F. He,[3] L. J. Wang,[3] H. Q. Ni,[3] Z. C. Niu,[3] and A. Muller[1,*]

[1]*Department of Physics, University of South Florida, Tampa, Florida 33620, USA*

[2]*University of Texas at Austin, Austin, Texas 78712, USA*

[3]*Institute of Semiconductors, Chinese Academy of Sciences, Beijing 100083, P.R. China*

(Received 2 April 2012; revised manuscript received 1 June 2012; published 19 June 2012)

We analyze the light scattered by a single InAs quantum dot interacting with a resonant continuous-wave laser. High-resolution spectra reveal clear distinctions between coherent and incoherent scattering, with the laser intensity spanning more than four orders of magnitude. We find that the fraction of coherently scattered photons can approach unity under sufficiently weak or detuned excitation, ruling out pure dephasing as a relevant decoherence mechanism. We show how spectral diffusion shapes spectra, correlation functions, and phase coherence, concealing the ideal radiatively broadened two-level system described by Mollow.

DOI: 10.1103/PhysRevB.85.235315 PACS number(s): 78.67.Hc, 78.47.−p, 78.55.Cr

Like an isolated atom or ion, a semiconductor quantum dot (QD) "artificial atom" scatters monochromatic laser light incident upon it. For an ideal two-level system broadened by radiative decay at a rate κ, the spectral and temporal properties of the scattered photons are determined solely by the laser detuning from resonance, $\Delta\omega$, and by the Rabi frequency, Ω. In seminal work, Mollow showed that when $\Omega \ll \kappa$, most of the light is scattered *coherently*, i.e., elastically, whereas it is otherwise dominated by resonance fluorescence.[1] Moreover, when the scattered light originates from a single two-level system it exhibits photon antibunching, *for any value of* Ω *and* $\Delta\omega$.[2]

Probing and controlling quantum phase coherence is at the core of quantum information science, and semiconductor QDs are well suited for investigating quantum coherence in solids at optical frequencies.[3] In this context, resonant light scattering in QDs has been of special interest and has emerged as a promising resource for the generation of highly ideal single-photon states.[4] Milestone demonstrations include oscillatory field correlations,[5] Mollow triplets,[6–8] photon antibunching,[6] and cascaded photon emission.[9] Nevertheless, the theoretical modeling of these experimental observations has necessitated the inclusion of a phenomenological dephasing time, T_2, in general smaller than $2T_1$, where $T_1 = 1/\kappa$ is the radiative lifetime.[5–9] Moreover, *coherent* scattering—as opposed to incoherent scattering, which causes resonance fluorescence—has remained largely unexplored. A more detailed experimental investigation clarifying the role of decoherence in the context of resonant light scattering is all the more timely given recent proposals of using coherent scattering for the generation of indistinguishable photons;[10,11] theory predicts that dephasing reduces the fraction of coherently scattered photons from unity, regardless of Ω and $\Delta\omega$. Here we combine high-resolution spectroscopy (35 MHz), photon correlations, and phase-coherence measurements to obtain clear distinctions between coherent and incoherent scattering. We show that the previously observed nonideal linewidth and correlation functions are due to the fluctuation of the QD resonance frequency on a time scale longer than T_1, resulting in an apparent broadening of the lineshape. On the other hand, at the relevant time scale of quantum evolution, the system is close to an ideal two-level system with negligible pure dephasing, as described by Mollow[1] and as expected from four-wave mixing measurements on QD ensembles.[12,13] We extend Mollow's theory to include spectral diffusion in the form of inhomogeneous broadening and provide a complete picture of resonant light scattering in semiconductor QDs.

We probe QDs grown by molecular beam epitaxy at the center of a planar optical microcavity. QDs of this type have been investigated extensively due to their atom-like spectra[3] and long dephasing times.[12] The QD sample was grown using a solid source VEECO Gen-II molecular beam epitaxy (MBE) system on a semi-insulating GaAs (100) substrate with a 12-pair top and 20-pair bottom $Al_{0.9}Ga_{0.1}As$/GaAs distributed Bragg reflector. The substrate rotation was stopped during MBE growth of InAs layers to obtain a QD density varying uniformly from 10^9 to $10^8/cm^2$.[14] The dominant vertical cavity mode is centered around $\lambda \approx 925$ nm. The sample was maintained at a temperature of 3.8 K in a closed-cycle cryostat and the QD emission was collected by an *in situ* high-numerical-aperture aspheric lens [Fig. 1(a)]. To excite a QD resonantly and discriminate the resonant scattering signal from stray laser light, an orthogonal excitation/detection geometry was used.[5] The detected light was coupled into a single-mode fiber without prior filtering or cross-polarized excitation/detection. For coarse spectral analysis of the emitted light a grating spectrometer with a cooled charge-coupled device camera was employed. For high-resolution spectral measurements we used a scanning Fabry-Perot interferometer with a free spectral range of 4.2 GHz and a finesse of 120 in conjunction with a single-photon counting detector. The excitation source was a diode laser continuously tunable over a range of several GHz. We have probed a number of single QDs and found very similar behavior, although the data presented here are from one specific QD.

Figure 1(b) shows the power spectrum of this QD under resonant laser excitation, recorded with a spectrometer with ≈10-GHz resolution. Although the main emission line is not resolved in this measurement, a broadband emission around it can be clearly identified. As is well known from experimental photoluminescence (PL) measurements,[15] four-wave mixing studies,[12,13] and theoretical calculations of resonance

 ©2012 American Physical Society

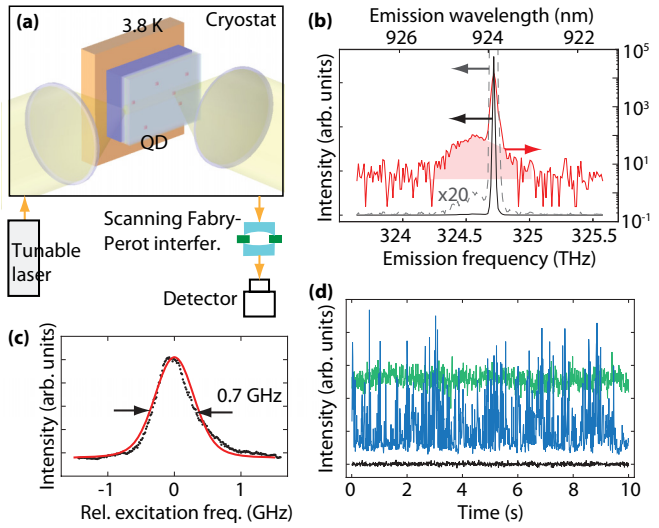

FIG. 1. (Color online) (a) Schematic of experimental setup. (b) QD emission spectrum, recorded with a grating spectrometer under resonant laser excitation as is [solid (black) trace], 20× magnified [dashed (gray) trace], and on a logarithmic scale [solid (red) trace] to visualize the phonon broadband. (c) QD excitation spectrum. (d) Spectrally integrated intensity of scattered light as a function of time showing flickering (dark blue trace) that is inhibited when an additional weak auxiliary laser is added (light green trace). The black trace was recorded with the auxiliary laser only.

fluorescence spectra,[16] this broad emission originates from fast scattering processes with acoustic phonons. Although at 3.8 K [Fig. 1(b)] this phonon scattering "pedestal" is highly asymmetric, it becomes more symmetric and prominent with increasing temperature.[12,15,16] In Fig. 1(b) about 5% of light is emitted into this broad band, thus at liquid He temperature, as much as ≈95% of light may be scattered coherently, irrespective of Ω and $\Delta\omega$.

Figure 1(c) shows the QD excitation spectrum at an excitation intensity below the saturation intensity, obtained by scanning the laser across the QD resonance frequency while collecting the scattered light. The full width at half-maximum (FWHM) of the resonance is about 0.7 GHz. Although in four-wave mixing studies the zero-phonon linewidth has been shown to be limited by radiative decay to about 170 MHz,[12,13] PL linewidths and/or resonantly measured single QD excitation linewidths are usually found to lie in the range of 500 MHz to several gigahertz.[5–11,17,19–21] The additional "apparent" broadening is due to spectral diffusion, a process by which the QD transition frequency is randomly shifted during the measurement.[17] This shift is thought to originate from a fluctuating charge environment of the QD that occurs on a time scale that is long compared to the radiative decay process. In PL measurements spectral diffusion is manifested in the form of long-time photon correlations and blinking.[22] In resonant scattering experiments the existence of charge fluctuations is evidenced by flickering[23] and by the fact that many resonances identified in PL as neutral exciton transitions generate little or no resonance fluorescence unless a weak background lighting is present.[20] It has been proposed that a Coulomb blockade effect is at the origin of this resonant emission quenching.[20] Flickering of the resonant scattering signal is directly observed when no external nonresonant lighting is present, as shown in Fig. 1(d), consistent with spectral diffusion.[24] The flickering can be inhibited on the measurement time scale (∼10 ms) by an auxiliary nonresonant light source (here a laser at $\lambda = 660$ nm) that is so weak that, by itself, it generates negligible PL [Fig. 1(d)]. We speculate that the effect of this auxiliary laser is to change the time scale of the flickering by neutralization of surrounding charges. Spectral diffusion is also commonly observed for QDs in nanostructures, where it is associated with the proximity of etched surfaces.[25]

In order to distinguish experimentally between coherent and incoherent scattering it is necessary to analyze the scattered light spectrally with a resolution better than κ. For a two-level system with natural resonance frequency ω_0, exposed to a monochromatic field of frequency ω, the power spectrum of the scattered light takes the analytic form, given by Mollow,[1]

$$\tilde{g}(\nu,\omega,\omega_0) = 2\pi|\alpha_\infty|^2\delta(\nu-\omega) + \bar{n}_\infty\kappa\Omega^2\frac{(\nu-\omega)^2+\Omega^2/2+\kappa^2}{|f(i(\nu-\omega))|^2}, \quad (1)$$

where ν is the emission frequency, and the only source of broadening is a decay of the upper state to the lower state at a rate κ due to spontaneous emission. The first term corresponds to photons scattered coherently, while the second term describes the resonance fluorescence. The laser detuning $\Delta\omega = \omega - \omega_0$ enters through the polynomial function f, the steady-state population inversion $\bar{n}_\infty$, and the steady-state quantum mechanical expectation value of the two-level coherence, α_∞, given in Ref. 1 and in the Appendix. Note that the function $\tilde{g}(\nu,\omega,\omega_0)$ is always symmetric around $\nu = \omega$ (not $\nu = \omega_0$), unlike spectra of dressed states populated nonresonantly.[18,26]

Figure 2(a) shows maps of the scattered light as a function of emission and excitation frequency, for various values of the Rabi frequency. The latter was varied by varying the laser intensity. As expected from Eq. (1), when $\Omega \ll \kappa$ [leftmost map in Fig. 2(a)], the emission resonance linewidth is much less than κ. It is limited here by the resolution of our scanning Fabry-Perot interferometer (35 MHz) but is expected to be as narrow as the laser linewidth (∼1 MHz). With increasing Ω the resonance fluorescence eventually dominates in the form of the Mollow triplet, composed of three peaks with a FWHM that is of the order of κ [middle and rightmost maps in Fig. 2(a)].

In order to identify the dominant effects on the QD two-level system due to its solid-state environment, we make a side-by-side comparison of our experimental data in Fig. 2(a) with spectral maps obtained from three theoretical models, displayed in Figs. 2(b)–2(d). In all cases, we assume a radiative decay, $\kappa/2\pi = 180$ MHz, which is consistent with typical radiative lifetimes [$\tau = 1/(2\pi \times 180\ \text{MHz}) = 0.9$ ns] for InAs QDs. We include spectral diffusion by integrating Eq. (1) over all possible (random) detunings to obtain

$$I(\nu,\omega,\omega_0) \propto \int \tilde{g}(\nu,\omega,\omega_0')e^{-(\omega_0'-\omega_0)^2/2\sigma^2}d\omega_0', \quad (2)$$

where we assume a Gaussian distribution of QD resonance frequencies due to spectral diffusion with FWHM $s \approx 2.355\sigma$. While spectral diffusion may manifest at different time

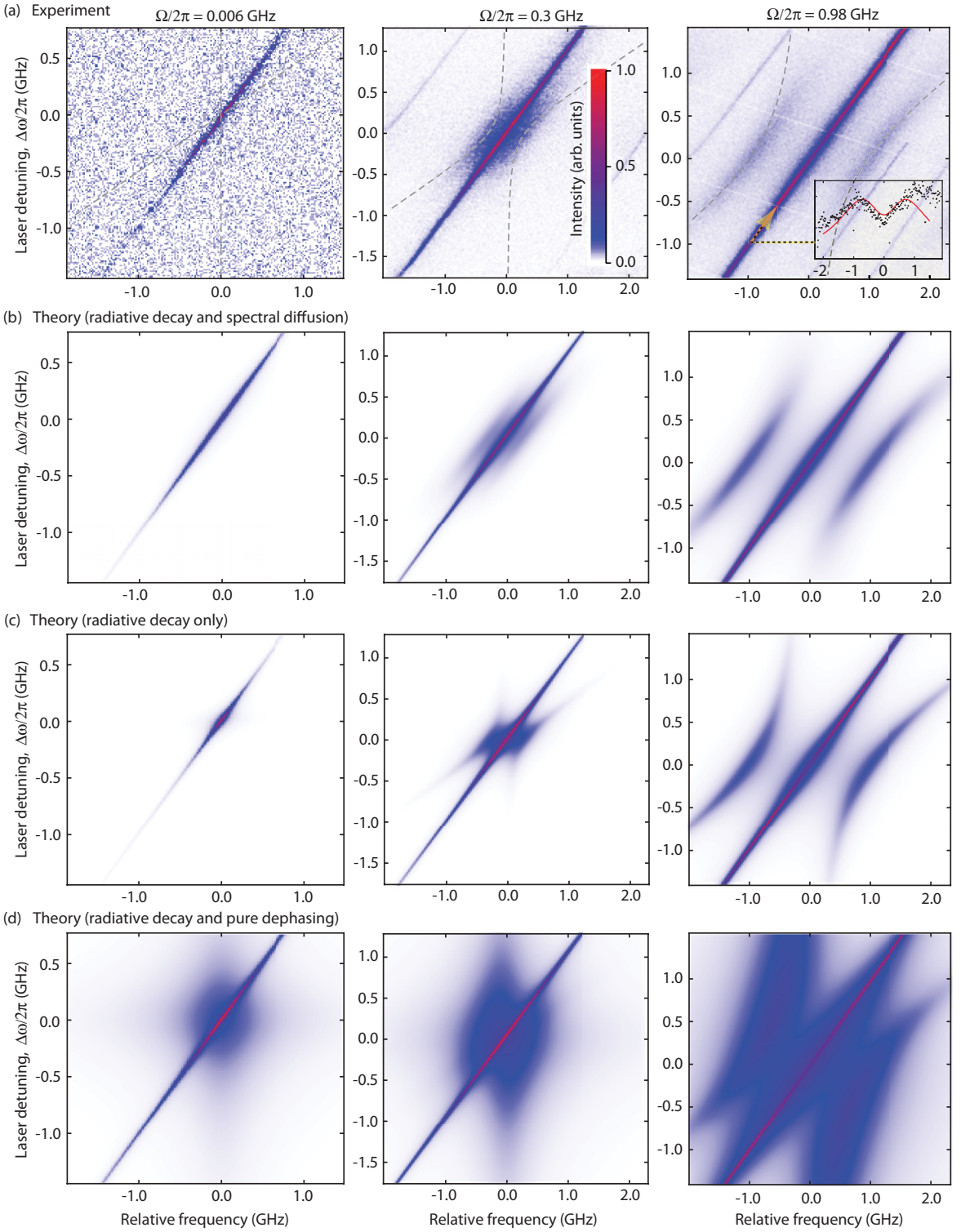

FIG. 2. (Color online) (a) Maps of scattered light intensity as a function of detection frequency (abscissas) and excitation frequency (ordinates) relative to the QD transition frequency, for three values of the Rabi frequency. Each panel was recorded in 200 s. At $\Omega/2\pi = 0.13$ GHz the detector count rate was 3×10^5 s^{-1} at the input of the Fabry-Perot interferometer. Ddashed lines indicate the location of the eigenfrequencies of the coupled laser/QD system. Inset: The line section $\nu = \omega$ together with the corresponding theoretical curve, obtained from Eq. (2). The faint diagonal lines parallel to the $\nu = \omega$ section are due to the residual transmission at high-order modes of the Fabry-Perot interferometer and satellite modes of the laser. (b) Theoretical maps Eq. (2) corresponding to a radiatively broadened two-level system subject to spectral diffusion. (c) Theoretical maps Eq. (1) representing an ideal, radiatively broadened two-level system. (d) Theoretical maps Eq. (A11) representing a two-level system subject to radiative decay and to pure dephasing at a rate γ. γ is chosen so as to obtain the excitation linewidth in Fig. 1(c).

scales,[27] we assume here that this time scale is long compared to the radiative decay time. We also neglect any influence of dark excitonic states.[28] To account for finite apparatus resolution we replace the δ function in Eq. (1) with a normalized Lorentzian with an FWHM equal to 35 MHz. Figure 3(b) shows spectral maps obtained using Eq. (2) with $s/2\pi = 0.7$ GHz, chosen to coincide with the measured excitation linewidth in Fig. 1(c), which is also typical for InAs QDs.[5–11,17,19–21,23] In comparison, Fig. 2(c) shows spectral maps obtained using Eq. (1), clearly not agreeing as well with the experimental data in Fig. 2(a) and highlighting the subtle effects of the spectral diffusion process. In Fig. 2(d) we further show the case when pure dephasing is present instead of spectral diffusion, as was assumed in previous studies.[5,6] The most general theoretical expressions for the power spectrum for the latter case are derived in the Appendix. The pure dephasing rate, γ, was chosen to yield the observed excitation linewidth [Fig. 1(c)]. As is evident from this comparison, pure dephasing does not play a major role at the measurement temperature since it would give rise to rather different observations. In particular, the absence of broad emission superimposed on the leftmost spectral map in Fig. 2(a) is an unequivocal indication that dephasing is not a relevant broadening process here.

For a quantitative analysis we recorded a series of spectra at exact resonance ($\Delta\omega = 0$) with a sufficiently high signal-to-noise ratio for precise comparison with theory (Fig. 3). The same information is displayed on both linear (left) and logarithmic (right) ordinate scales. The theoretical traces were obtained using Eq. (2) with the same parameters as in Fig. 2(b), and only a common scale factor was permitted for all traces. Short-dashed and long-dashed (red) lines correspond to the total and the incoherent scattered light intensity, respectively, and the shaded (red) area indicates the coherently scattered light. As shown in the figure, there is excellent agreement between the experimental data and the theoretical expression of Eq. (2) evaluated numerically, considering that the excitation laser intensity spans more than four orders of magnitude. Since at the largest Ω in Fig. 3 the central peak continues to grow, some amount of light is, at that point, originating from other scatterers, perhaps neighboring detuned QDs. Nonetheless, when $\Omega/2\pi = 0.49$ GHz, we can estimate that more than 90% of the detected light originates from scattering off the QDs probed.

Photon statistics of the scattered light, shown in Fig. 4(a) below saturation (left panel), near saturation (middle panel), and above saturation (right panel), corroborate this via the observation of photon antibunching. Photon correlation measurements were performed with a Hanbury-Brown and Twiss setup[29] that uses a 2×2 fiber coupler and two fiber-coupled avalanche photon detectors. The detectors are nominally identical to those used in Ref. 6 and thus an identical instrument response function (IRF) was assumed. We show the raw unprocessed normalized data as well as the theoretical normalized second-order correlation function in the presence of spectral diffusion, $g^{(2)}_{\mathrm{SD}}(t)$, convolved with the IRF.[6] It is the IRF, not stray background light, that causes the dip to rise above 0 near $t = 0$. $g^{(2)}_{\mathrm{SD}}(t)$ is computed identically to Eq. (2), replacing $\tilde{g}(\nu,\omega,\omega_0')$ under the integral with $g^{(2)}(t,\omega,\omega_0')\bar{n}_\infty/\bar{n}_\infty(\omega = \omega_0)$, where $g^{(2)}(t,\omega,\omega_0')$ is the

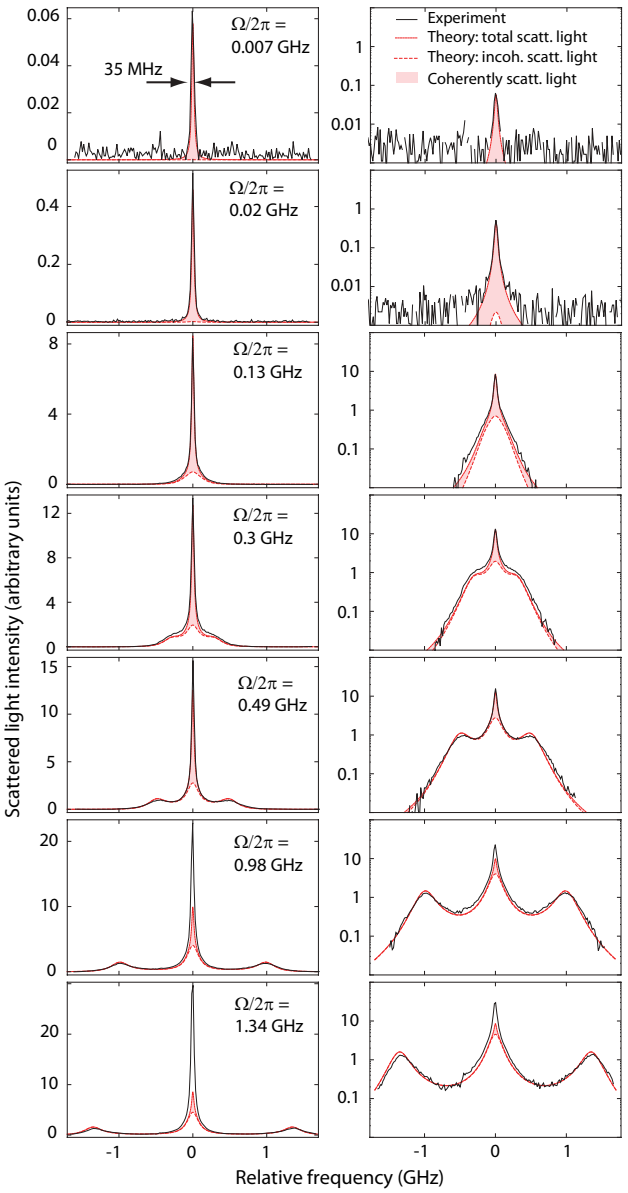

FIG. 3. (Color online) Power spectrum of light scattered by the QD at exact resonance ($\Delta\omega = 0$) represented on a linear (left) and a logarithmic (right) ordinate scale, for a range of Rabi frequencies. Each spectrum was recorded in 60 s. The theoretical curve [dashed (red) line] was obtained by numerical evaluation of Eq. (2). The shaded (red) area corresponds to coherently scattered light, which dominates whenever $\Omega \lesssim \kappa$. If pure dephasing had a significant role in the scattering process, a broader feature would always be visible, even when $\Omega \ll \kappa$.

normalized correlation function for the ideal two-level system. Above saturation, Rabi oscillations, the time-domain analog of the side bands in Fig. 2, are seen.[6]

Spectral diffusion significantly alters the spectral and temporal characteristics of the scattering process compared to the ideal two-level system. Figure 4(b) shows the total normalized scattered light intensity as a function of the Rabi frequency for the parameters used in Fig. 3. using Eq. (2) [solid (red) trace] and Eq. (1) [solid (blue) trace]. Correspondingly, the dashed lines of the same color represent the fraction of

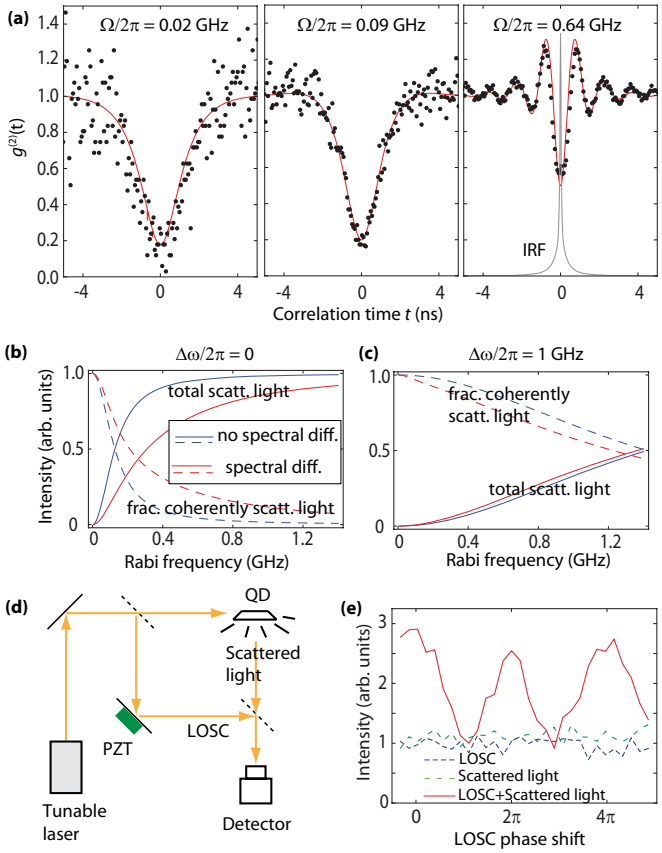

FIG. 4. (Color online) (a) Photon statistics of scattered light for three Rabi frequencies. When $\Omega > \kappa$, Rabi oscillations appear. (b) Plot of the total scattered light intensity [solid (red) trace] and the fraction of coherently scattered light intensity [dashed (red) trace], using the same parameters as in Fig. 3. For comparison the same, but not including spectral diffusion, are plotted in blue. (c) Same as (b), but with a laser detuned by $\Delta\omega/2\pi = 1$ GHz. (d) Measurement of mutual phase coherence between the coherently scattered light and a local oscillator (LOSC) by interferometry. (e) Intensity of light at the output of the beam splitter in (d) as a function of the LOSC phase.

the intensity of coherently scattered light alone. The same are plotted in Fig. 4(c), but under significant laser detuning. A signature effect of the spectral diffusion is to cause an *increase* in the fraction of photons scattered coherently, as would any source of inhomogeneous broadening. At large values of Ω, more light is actually scattered coherently with the laser off-resonance than with the laser at exact resonance. This is shown in Fig. 4(c) but is also directly visible in the bottom map in Fig. 2, where a minimum occurs along the line $\nu = \omega$ at resonance (inset).

Finally, we examine the phase coherence between the laser and the scattered light (below saturation) by combining the scattered light with a local oscillator (LOSC) signal at a beam splitter. We measure the fringe contrast obtained when varying the LOSC phase with a piezoelectric actuator [Fig. 4(d)]. The fringe contrast we obtain here is ≈40% as shown in Fig. 4(e), which can be understood by spectral diffusion, which causes large fluctuations in photon flux at the beam splitter. In theory we expect spectral diffusion to reduce the fringe contrast (visibility) by a factor of order $\kappa/s \approx 0.25$.

In summary, we have carried out high-resolution measurements of the light scattered coherently and incoherently by a single InAs QD, revealing in great detail how the scattering process evolves over more than four orders of magnitude of excitation laser intensity. The simple inclusion in Mollow's theory of spectral diffusion as a source of inhomogeneous broadening does faithfully reproduce both our observed spectra and photon correlation and phase-coherence measurements. The insight that an apparent broadening rather than pure dephasing predominantly affects the scattering process has important implications for future use of QDs, for example, in quantum repeaters.[30] There we expect spectral diffusion to reduce the photon flux, without, however, limiting two-photon indistinguishability.[8] The temporal flickering of the resonant scattering signal associated with the spectral diffusion may be reduced in future improved structures. For example, it may be possible to control the time scale for this flickering by placing QDs in charge-tunable devices. Overall our work offers a complete picture of resonant light scattering relevant to a wide variety of solid-state nanostructures.

ACKNOWLEDGMENTS

The authors acknowledge financial support from the National Science Foundation (Grant Nos. NSF DMR-0906025 and CMMI-0928664) and the National Natural Science Foundation of China (Grant No. 90921015).

APPENDIX: POWER SPECTRUM IN THE PRESENCE OF PURE DEPHASING AND DETUNING

Using the same notation as in Ref. 1, we provide an expression for the power spectrum of the light scattered by a two-level system subject to an incident monochromatic laser, when including an additional off-diagonal decay (pure dephasing) rate γ. Unlike in Refs. 5 and 6, we further assume that the detuning is not 0, i.e., $\Delta\omega \neq 0$.

The optical Bloch equations in the rotating-wave approximation read

$$\frac{d}{dt}\mathbf{R}(t) = \mathbf{M}\cdot\mathbf{R}(t), \tag{A1}$$

in which

$$\mathbf{M} = \begin{pmatrix} -\kappa & -i\Omega/2 & i\Omega/2 & 0 \\ -i\Omega/2 & -\kappa/2-\gamma+i\Delta\omega & 0 & i\Omega/2 \\ i\Omega/2 & 0 & -\kappa/2-\gamma-i\Delta\omega & -i\Omega/2 \\ \kappa & i\Omega/2 & -i\Omega/2 & 0 \end{pmatrix} \tag{A2}$$

and

$$\mathbf{R}(t) = \begin{pmatrix} n(t) \\ \alpha(t) \\ \alpha^*(t) \\ m(t) \end{pmatrix}. \tag{A3}$$

Here $n(t) = \mathrm{Tr}\rho(t)a^\dagger a, \alpha(t) = \mathrm{Tr}\rho(t)a, \alpha^*(t) = \mathrm{Tr}\rho(t)a^\dagger$, and $m(t) = \mathrm{Tr}\rho(t)aa^\dagger$, where a, $a^\dagger$, and ρ are the lowering, raising, and density operators, respectively. The diagonal and off-diagonal damping terms $\frac{1}{T_1} = \kappa$ and $\frac{1}{T_2} = \gamma + \kappa/2$, respectively, have been included using the usual master equation. Equation (A1) has the steady-state solution

$$\alpha_\infty = \frac{i\Omega}{4} \frac{\kappa + 2\gamma + 2i\Delta\omega}{\Delta\omega^2 + (\kappa + 2\gamma)(\kappa + 2\gamma + 2\Omega^2/\kappa)/4} \tag{A4}$$

and

$$n_\infty = \frac{\Omega^2}{4\kappa} \frac{\kappa + 2\gamma}{\Delta\omega^2 + (\kappa + 2\gamma)(\kappa + 2\gamma + 2\Omega^2/\kappa)/4}. \tag{A5}$$

Following Mollow,[1] the power spectrum is obtained as the Fourier transform of the first-order correlation function, $g(\tau,t) \equiv \langle a^\dagger(t)a(t+\tau)\rangle$, in steady state ($t \to \infty$), as

$$\tilde{g}(\nu) \equiv \int_{-\infty}^{\infty} g(\tau)e^{i\nu\tau}d\tau = 2\mathrm{Re}(\hat{g}(-i\nu)), \tag{A6}$$

where ν is the angular frequency of the scattered light, and $\hat{g}(s)$ is the Laplace transform of $g(\tau)$. In order to calculate $g(\tau)$ we make use of the quantum regression theorem,[31] which states that for an operator $\mathcal{O}$ whose expectation value is known to evolve from time t to time $t+\tau$ as

$$\langle \mathcal{O}(t+\tau)\rangle = \sum_j a_j(\tau)\langle \mathcal{O}_j(t)\rangle, \tag{A7}$$

the two-time correlation function $\langle \mathcal{O}_i(t)\mathcal{O}(t+\tau)\mathcal{O}_k(t)\rangle$ can be calculated as a function of single time expectation values as follows:

$$\langle \mathcal{O}_i(t)\mathcal{O}(t+\tau)\mathcal{O}_k(t)\rangle = \sum_j a_j(\tau)\langle \mathcal{O}_i(t)\mathcal{O}_j(t)\mathcal{O}_k(t)\rangle. \tag{A8}$$

Given that the solution of Eq. (A1) can be written as

$$\mathbf{R}(t+\tau) = e^{\mathbf{M}\tau} \cdot \mathbf{R}(t), \tag{A9}$$

we obtain

$$g(\tau) = \left(e^{\mathbf{M}\tau}|_{2,2}n_\infty + e^{\mathbf{M}\tau}|_{2,4}\alpha^*_\infty\right)e^{-i\omega\tau - \delta_{\mathrm{FP}}\tau/2}. \tag{A10}$$

To account for the limited resolution, δ_{FP}, of our scanning Fabry-Perot interferometer, we have multiplied the correlation function by $e^{-\delta_{\mathrm{FP}}\tau/2}$ ($\tau \geqslant 0$). Computing (A6) requires finding the Laplace transform of (A10), which in turn involves computing the matrix $(\mathbb{I}s - \mathbf{M})^{-1}$, where $\mathbb{I}$ is the 4×4 identity matrix. We finally obtain

$$\begin{aligned}\tilde{g}(\nu) = 2\mathrm{Re}((&\mathbb{I}(-i\nu + i\omega + \delta_{\mathrm{FP}}/2) - \mathbf{M})^{-1}|_{2,2}n_\infty \\ &+ (\mathbb{I}(-i\nu + i\omega + \delta_{\mathrm{FP}}/2) - \mathbf{M})^{-1}|_{2,4}\alpha^*_\infty),\end{aligned} \tag{A11}$$

which, for the special case $\gamma = 0$ and $\delta_{\mathrm{FP}} = 0$, reduces to the expression

$$\tilde{g}(\nu) = 2\pi|\alpha_\infty|^2\delta(\nu - \omega) + \bar{n}_\infty\kappa\Omega^2\frac{(\nu-\omega)^2 + \Omega^2/2 + \kappa^2}{|f(i(\nu-\omega))|^2} \tag{A12}$$

given by Mollow [Eq. (1)], where $f(s) = s^3 + 2\kappa s^2 + (\Omega^2 + (\Delta\omega)^2 + (5/4)\kappa^2)s + \kappa(\frac{1}{2}\Omega^2 + (\Delta\omega)^2 + \frac{1}{4}\kappa^2)$.

*Corresponding author: mullera@usf.edu

[1] B. R. Mollow, Phy. Rev. **188**, 1969 (1969).

[2] C. Cohen-Tannoudji, J. Dupont-Roc, and G. Grynberg, *Atom-Photon Interactions* (John Wiley & Sons, New York, 1992).

[3] M. Bayer, O. Stern, P. Hawrylak, S. Fafard, and A. Forchel, Nature **405**, 923 (2000).

[4] A. Kiraz, M. Atatüre, and A. Imamoğlu, Phys. Rev. A **69**, 032305 (2004).

[5] A. Muller, E. B. Flagg, P. Bianucci, X. Y. Wang, D. G. Deppe, W. Ma, J. Zhang, G. J. Salamo, M. Xiao, and C. K. Shih, Phys. Rev. Lett. **99**, 187402 (2007).

[6] E. B. Flagg, A. Muller, J. W. Robertson, S. Founta, D. G. Deppe, M. Xiao, W. Ma, G. J. Salamo, and C. K. Shih, Nat. Phys. **5**, 203 (2009).

[7] N. Vamivakas, Y. Zhao, C.-Y. Lu, and M. Atatüre, Nat. Phys. **5**, 198 (2009).

[8] S. Ates, S. M. Ulrich, S. Reitzenstein, A. Löffler, A. Forchel, and P. Michler, Phys. Rev. Lett. **103**, 167402 (2009).

[9] A. Ulhaq, S. Weiler, S. M. Ulrich, R. Robach, M. Jetter, and P. Michler, Nat. Photon. **6**, 238 (2012).

[10] H. S. Nguyen, G. Sallen, C. Voisin, Ph. Roussignol, C. Diederichs, and G. Cassabois, Appl. Phys. Lett. **99**, 261904 (2011).

[11] C. Matthiesen, A. N. Vamivakas, and M. Atatüre, Phys. Rev. Lett. **108**, 093602 (2012).

[12] P. Borri, W. Langbein, S. Schneider, and U. Woggon, Phys. Rev. Lett. **87**, 157401 (2001).

[13] W. Langbein, P. Borri, U. Woggon, V. Stavarache, D. Reuter, and A. D. Wieck, Phys. Rev. B **70**, 033301 (2004).

[14] S. Huang, Z. Niu, H. Ni, Y. Xiong, F. Zhan, Z. Fang, and J. Xia, J. Cryst. Growth **301**, 751 (2007).

[15] L. Besombes, K. Kheng, L. Marsal, and H. Mariette, Phys. Rev. B **63**, 155307 (2001).

[16] K. J. Ahn, J. Förstner, and A. Knorr, Phys. Rev. B **71**, 153309 (2005).

[17] A. Högele, S. Seidl, M. Kroner, K. Karrai, R. J. Warburton, B. D. Gerardot, and P. M. Petroff, Phys. Rev. Lett. **93**, 217401 (2004).

[18] G. Jundt, L. Robledo, A. Högele, S. Fält, and A. Imamoğlu, Phys. Rev. Lett. **100**, 177401 (2008).

[19] X. Xu, B. Sun, P. R. Berman, D. G. Steel, A. S. Bracker, D. Gammon, and L. J. Sham, Science **317**, 929 (2007).

[20] H. S. Nguyen, G. Sallen, C. Voisin, Ph. Roussignol, C. Diederichs, and G. Cassabois, Phys. Rev. Lett. **108**, 057401 (2012).

[21] S. M. Ulrich, S. Ates, S. Reitzenstein, A. Lffler, A. Forchel, and P. Michler, Phys. Rev. Lett. **106**, 247402 (2011).

[22]C. Santori, D. Fattal, J. Vučković, G. S. Solomon, E. Waks, and Y. Yamamoto, Phys. Rev. B **69**, 205324 (2004).
[23]C. Latta, A. Högele, Y. Zhao, A. N. Vamivakas, P. Maletinsky, M. Kroner, J. Dreiser, I. Carusotto, A. Badolato, D. Schuh, W. Wegscheider, M. Atature, and A. Imamoglu, Nat. Phys. **5**, 758 (2009).
[24]R. G. Neuhauser, K. T. Shimizu, W. K. Woo, S. A. Empedocles, and M. G. Bawendi, Phys. Rev. Lett. **85**, 3301 (2000).
[25]A. Majumdar, E. D. Kim, and J. Vučković, Phys. Rev. B **84**, 195304 (2011).
[26]A. Muller, W. Fang, J. Lawall, and G. S. Solomon, Phys. Rev. Lett. **101**, 027401 (2008).
[27]I. Favero, A. Berthelot, G. Cassabois, C. Voisin, C. Delalande, Ph. Roussignol, R. Ferreira, and J. M. Gérard, Phys. Rev. B **75**, 073308 (2007).
[28]M. Bayer, O. Stern, A. Kuther, and A. Forchel, Phys. Rev. B **61**, 7273 (2000).
[29]P. Michler, A. Kiraz, C. Becher, P. M. Petroff, E. Hu, and A. Imamoglu, Science **290**, 2282 (2000).
[30]E. B. Flagg, A. Muller, S. V. Polyakov, A. Ling, A. Migdall, and G. S. Solomon, Phys. Rev. Lett. **104**, 137401 (2010).
[31]M. O. Scully and M. S. Zubairy, *Quantum Optics* (Cambridge University Press, Cambridge, 1997).